# CONSTRUCTION AND TEST OF A CYLINDRICAL CERAMIC TRANSDUCER OF A PRESTRESSED SEGMENTED DESIGN

FRED S. UNDERWOOD

# CONSTRUCTION AND TEST OF A CYLINDRICAL CERAMIC TRANSDUCER OF A PRESTRESSED SEGMENTED DESIGN

* * * * *

FRED S. UNDERWOOD

# CONSTRUCTION AND TEST OF A CYLINDRICAL CERAMIC TRANSDUCER OF A PRESTRESSED SEGMENTED DESIGN

by

FRED S. UNDERWOOD
Lieutenant, United States Navy

Submitted in partial fulfillment of the requirements for
the degree of
MASTER OF SCIENCE
in
ENGINEERING ELECTRONICS
United States Naval Postgraduate School
Monterey, California
1963

# CONSTRUCTION AND TEST OF A CYLINDRICAL CERAMIC TRANSDUCER OF A PRESTRESSED SEGMENTED DESIGN

by

Fred S. Underwood

This work is accepted as fulfilling
the thesis requirements for the degree of

MASTER OF SCIENCE
in
ENGINEERING ELECTRONICS

from the
United States Naval Postgraduate School

ABSTRACT

In an effort to obtain more acoustic power from a given transducer which is subject to an input voltage limitation, it is desirable to drive the most active ceramic transducer material in the mode in which the coupling coefficient is largest. To achieve this end a transducer was constructed from a Lead Zirconate-Titanate ceramic by molding segments of the material, gluing them together to form a cylinder, and then circumferentially prestressing the cylinder. The construction techniques, the equivalent circuit, and the changes in parameters of the transducer as a result of construction steps as well as some interesting phenomena observed during the high level testing of the transducer are discussed.

The writer wishes to express his appreciation for the assistance and encouragement given him by Mr. D.B. Connelly, and Mr. T.C. Madison of the Transducers and Techniques Section, Sonar Department, Heavy Military Electronics Division, General Electric Company, Syracuse New York.

TABLE OF CONTENTS

LIST OF ILLUSTRATIONS

Table of Symbols and Abbreviations

The following symbols and abbreviations are used in the text of this paper:

| Symbol | value | meaning |
|---|---|---|
| $A_e$ | | Area of exterior face of one segment (square meters) |
| $A_r$ | | Cross-sectional area of the rough transducer (square meters) |
| $A_s$ | | Cross-sectional area of the sanded transducer (square meters) |
| C | | Motional Capacitance of the equivalent circuit (farads) |
| $C_m$ | | Velocity of sound in the medium (meters/second) |
| $C_o$ | | Dielectric capacitance across the input to the transducer (farads) |
| $d_{33}$ | $2.1(10^{-10})$ | Piezo-electric strain coefficient (meters/volt) |
| $E_y$ | | Drive voltage of the transducer (volts) |
| $F_c$ | | Circumferential force (newtons) |
| $F_r$ | | Radial force (newtons) |
| $F_y$ | | Force applied in the direction of polarization (newtons) |
| H | $7.6(10^{-2})$ | Height of transducer (meters) |
| K | .62 | Coupling coefficient |
| L | | Motional inductance in the equivalent circuit (henries) |
| $L_y$ | $1.25(10^{-2})$ | Mean distance between segment electrodes (meters) |

| Symbol | value | meaning |
|---|---|---|
| $L_1$ | 0.0135 | Length of base of truncated prism (meters) |
| $L_2$ | 0.0115 | Length of top of truncated prism (meters) |
| M | | Mass of the transducer (kilograms) |
| $M_p$ | | Mass of the potted transducer (kilograms) |
| $M_{ps}$ | | Mass of the prestressed transducer (kilograms) |
| $M_r$ | | Mass of the rough transducer (kilograms) |
| $M_s$ | | Mass of sanded transducer (kilograms) |
| N | 28.0 | Number of segments in the transducer |
| $P_c$ | | Pressure acting circumferentially on an axial cross-section of the transducer (newtons/square meter) |
| $P_r$ | | Pressure acting radially on the surface of the transducer (newtons/square meter) |
| Q | | Quality factor of the transducer |
| $R_m$ | | Internal motional losses of the equivalent circuit (ohms) |
| $R_{me}$ | | Mean radius of the cylindrical transducer (meters) |
| $R_o$ | | Dielectric losses across the input to the transducer (ohms) |
| $R_r$ | | Radiation losses to the medium (ohms) |

| Symbol | value | meaning |
|---|---|---|
| $R(f)$ | | Radiation losses due to internal loading (ohms) |
| $R_1$ | 0.0604 | Outside radius of the unsanded cylinder (meters) |
| $R_2$ | 0.05192 | Inside radius of unsanded cylinder (meters) |
| $S$ | | Compliance coefficient (square meters/newton) |
| $S_{33}$ | $1.32(10^{-11})$ | Compliance coefficient of PZT-4 (square meters/newton) |
| $S_y$ | $6.45(10^{-4})$ | Plated area of one bar (square meters) |
| $T$ | 0.0085 | Thickness of a segment (meters) |
| $X$ | | Dimension of a typical segment (meters) |
| $X(f)$ | | Radiation reactance due to internal loading (ohms) |
| $\epsilon_o$ | $8.85(10^{-12})$ | Permittivity of free space (farads/meter) |
| $\epsilon_y$ | 1300.0 | Free dielectric constant of PZT-4 |
| $\epsilon_y'$ | | Clamped dielectric constant of PZT-4 |
| $\partial\eta/\partial y$ | | Strain in the y direction (meters/meter) |
| $\Theta$ | 0.224 | Angle subtended by one segment (radians) |
| $\xi_c$ | | Circumferential displacement (meters) |
| $\xi_r$ | | Radial displacement (meters) |
| $\pi$ | 3.1415927 | |
| $\rho$ | 7500.0 | Density of PZT-4 (kilograms/cubic meter) |

| Symbol | value | meaning |
|---|---|---|
| $\rho_o$ | | Density of the medium (kilograms/cubic meter) |
| $\sigma_y$ | | Charge density on the electrodes (coulombs/square meter) |
| $\Phi$ | | Transformation factor (newtons/volt) |
| $\omega_r$ | | Resonant frequency (radians/second) |

1. Introduction

In modern transducer technology a continuing goal is to improve on the source level of a given transducer. It is generally accepted that there are two physical conditions which limit the amount of acoustic power that a transducer may radiate. These are:

a. Electric field limiting. The driving voltage is increased until either arc-over or dielectric break-down occurs between the driving electrodes.

b. Stress limiting. The motion of the material is of such magnitude that either the stresses in the material exceed the tensile strength of the material and the transducer shatters, or the heating from mechanical losses exceeds the cooling capacity and the transducer is destroyed.

If it is assumed that a given transducer is field limited, then it would be advantageous to utilize a material for construction which would have as high an electro-mechanical coupling coefficient as possible. The higher the coupling coefficient, the lower will be the electrical impedance at resonance, and therefore, for a given limiting voltage more current and more power may be used to drive the transducer, resulting in increased output power from the device.

Since the transducers, which are the subject of this paper, were intended as replacements for transducers currently in service, the criterion of frequency, shape, and size had been previously established. This left as a design problem, the maximization of output acoustic power. A design in which the transducer is circumferentially prestressed was concieved by Mr. D.B. Connelly and Mr. T.C. Madison. This prestressing should reduce the possibility that the transducer is stress limited thereby leaving the relatively simple problem of choosing a material and drive arrangement for maximum power output.

A Lead Zirconate-Titanate solid solution ($Pb_{0.94}Sr_{0.06}Zr_{0.53}Ti_{0.47}O_3$)[1] was chosen on the basis of its strong coupling coefficient in the parallel or $k_{33}$ mode of vibration. The large coupling coefficient ($k_{33}$=

1. R.Gerson, "Dependence of Mechanical Q and Young's Modulus of Ferroelectric Ceramics on Stress Amplitude", Jour.Acoust. Soc. Amer. Vol 32, No.10, p 1299, Table I, Oct 1960.

0.64)[1] of this material is in the class of that for Rochelle Salt, one of the most active piezo-electric materials known.

After choosing the material there remained the decision of method of drive to utilize the coupling coefficient to its fullest advantage. There are two obvious methods for exciting a cylinder in the circumferential mode, using the parallel mode of excitation.

The following procedure is used in the first method. The transducer may be striped (i.e. the transducer is partially plated with a conducting material. The electrodes are in the form of stripes parallel with the cylinder axis with the electrode on the outside and that on the inside of the hollow cylinder being electrically connected. The piezo-electric material is then polarized between adjacent stripes.) The primary advantage of striping is the simplicity of construction. Its outstanding disadvantages are: The stripes have a finite width which causes an appreciable portion of the piezo-electric material directly beneath the stripe to remain unpolarized and therefore not active; the non-uniform field distribution (see Fig. 1) causes the transducer to be field limited directly between electrodes while the remainder of the transducer contains an electric field strength well below the limiting level, and thus the full potential of the material is not realized.

In the second method of driving a cylindrical transducer circumferentially in the parallel mode is realized by using a segmented cylinder. (The cylinder is cut longitudinally into an even number of parts. The cut edges are plated and the individual pieces poled and then reassembled to form the cylinder.) The primary advantage in the segmented construc-

1. D. Berlincour, B. Jaffe, H. Jaffe, and H. H. A. Krueger, "Transducer Properties of Lead Titanate Zirconate Ceramics", I.R.E. Trans. on Ultrasonics Eng. Vol UE-7, No. 1, pp 1-6, Feb. 1960.

tion is the improvement in the field distribution pattern in the ceramic (see Fig. 2). The circumferential length of the electrode, approximately twice the thickness of the plated electrode plus the thickness of the binding agent, is small. Moreover, the piezo-electric material is not placed directly between two electrodes of the same potential as in the striped design, so that all of the ceramic in the transducer is active. Since the distance between the two electrodes is non-uniform the transducer will be field limited at the interior edge of the electrode while the rest of the ceramic remains below the limiting field level. However with the dimensions involved in the case considered here, when the interior edge is field limited the ceramic at the exterior edge of the electrode will be at 84% of the limiting field level. The outstanding disadvantage in using segmented transducer is the possible weakness of the bond which could cause the transducer to be severely stress limited. Another disadvantage of this type transducer is the complexity of its construction.

For this particular type of application the segmented type of construction was chosen to provide efficient circumferential exitation. It is the opinion of the designers and of the writer that the circumferential prestress applied is sufficient to remove, essentially, the possibility of stress limitation.

After the completion of construction of several of the transducers, tests were conducted to observe the effects of operating temperature and dynamic stress level on the various parameters of the transducer. The slope of the curve of resonant frequency versus temperature was positive until a temperature of $60^{\circ}$C. was reached where the slope passed through zero and from $60^{\circ}$C. on up to $105^{\circ}$C. the slope was negative. In the tests at high dynamic stress levels the work of Robert Gerson[1] for this transducer configuration was verified.

1. R. Gerson Op.Cit.

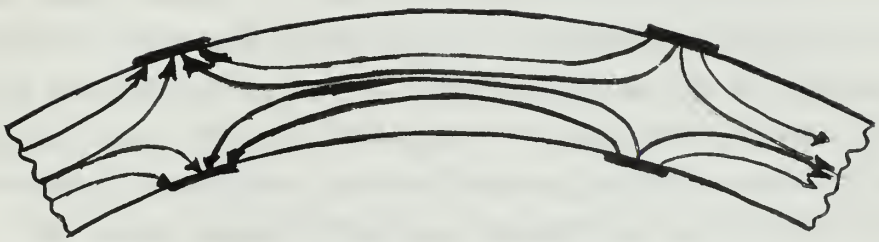

Figure 1. Electric field distribution in the ceramic cylinder with external plated electrodes

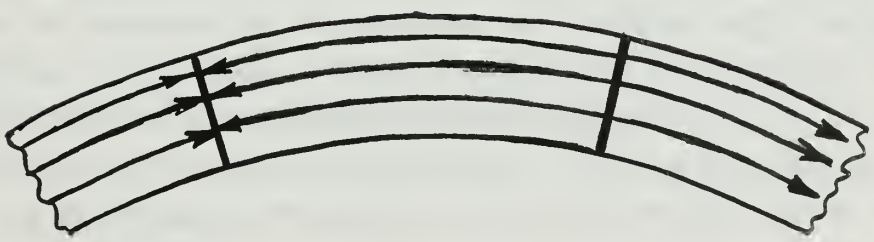

Figure 2. Electric field distribution in the ceramic segmented cylinder with internal plated electrodes

2. Construction of the Prestressed Segmented Cylindrical Transducers

The transducers, which are the subject of this paper, are composed of 28 segments cemented together to form a hollow cylinder. The individual segments are of a Lead Zirconate-Titanate ceramic composition. The segments are shaped in the form of a truncated prism with the dimensions as depicted in Fig. 3. Each individual bar is polarized between the sloping faces with a periodically reversing direct current potential at an elevated temperature, yet well below the Curie point of the compound. The exact applied potential, temperature and length of time to achieve polarization were considered to be proprietary in nature and were not made available to the writer. During the pressing of the ceramic, three indentations are made in the sloping faces for the attachment of electrodes. There are two indentations on one side and the remaining indentation on the other. During the poling process each bar is polarized in a manner such that the side with the two connections is always positive. This consistancy is utilized when the cylinder is assembled to assure that reverse polarized segments are not inserted in the cylinder. Prior to assemble, all of the segments are ultrasonically cleaned and the electrode leads are attached to the plated surfaces. A jig, consisting of two fiber-board rings, which have an outside diameter equal to the inside diameter of the completed transducer, separated by spacers, is used to hold the individual segments while they are being cemented. The adhesive agent used was "Epon-6" mixed with "Epon" curing agent "A" in accordance with the directions supplied by the manufacturer. After the 28 segments are in place they are clamped with a screw type hose clamp and the entire assembly is placed in the oven at a temperature of 60$^{o}$C. for a period of fourteen hours for curing.

After curing the assembled cylinder is removed from the jig, and the wiring is connected internally in such a manner that all of the elements are driven in parallel.

The cylinders are then circumferentially prestressed by wrapping with fiber glass. But, since the fiber glass strands tend to break when placed in tension and flexed across a sharp edge, it was decided to

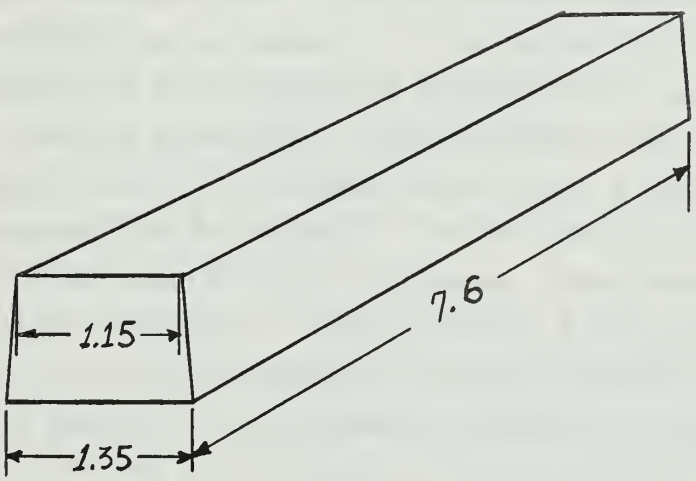


Figure 3. Ceramic bar used in construction of the segmented cylindrical transducer. (Dimensions are given in centimeters)

sand off the corners of the 28-sided polygon to make it an approximation to a cylinder. The transducer was mounted in a clamp and chucked in a lathe. Carborundum sand paper was used to round off the corners.

After sanding, strain guages were attached and prestressing was begun. The fiber glass was pulled by the cylinder mounted in the lathe from a braked drum which kept the fiber glass strainds under a constant tension of approximately nine pounds. The epoxy resin (Epon resin 815 with curing agent D) was applied by the lathe operator. From the strain guages installed the degree of prestress was calculated. Wrapping was continued until the desired degree of prestress was achieved. The transducer assembly was then placed in an oven to cure for fourteen hours at a temperature of $50^{\circ}C$.

To achieve the desired insulation when immersed in water, the transducer was potted in a polyurethane compound (Hysol RU 2085 resin with Hysol hardener 3500). The polyurethane compound was chosen both for its properties as an insulator as well as for the fact that the acoustic impedance of the compound is essentially the same as that of sea water. To pot the transducer a mold was built to the final shape desired, the polyurethane and hardener mixed under a vacuum and poured over the prestressed ring in the mold. The mold was placed in the oven for a period of eight hours at $80^{\circ}C$. for curing. This completed the construction of the transducer. During the test of one of the first of the transducers it was discovered that the oven curing did not completely cure the Epon-6 adhesive. Investigation revealed that proper curing was achieved by driving the transducer at resonance with a high input voltage. The dissipation in the transducer elevated the temperature while the dynamic stresses set up in the adhesive apparently accelerated the curing process. For the remainder of the transducers, curing was completed by driving them at resonance with an input power of approximately 100 watts until the temperature of the element was elevated to $105^{\circ}C$.

3. The Equivalent Circuit of the Segmented Cylindrical Transducer.

As in the case of any other electro-mechanical transducer, the segmented cylindrical transducer may be approximated in the vicinity of its resonant frequency by an equivalent circuit consisting of a motional series resonant branch paralleled by the components arising from the static or blocked transducer.

The equivalent circuit for this type of transducer is shown in Fig. 4.

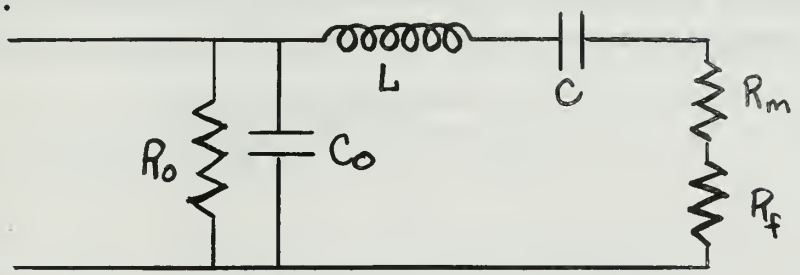


Figure 4. Equivalent circuit for an electro-mechanical transducer.

The quantities depicted in Fig. 4 are:

a. $C_o$ the static dielectric capacitance
b. $R_o$ the dielectric resistance
c. L the motional inductance
d. C the motional capacitance
e. $R_m$ the internal motional resistance
f. $R_f$ the coupled acoustic radiation resistance

The remainder of this section is concerned with a derivation of the algebraic expressions for the above listed equivalent circuit components, relating them to the various constants and dimensions of the transducer.

For two of the components, $R_o$ and $R_m$, the writer has been unable to derive or find an equation relating the observed properties of these components to the constants and dimensions of the transducer.

Experimental measurements revealed that the blocked conductance was almost zero, so that for the remainder of the paper $R_o$ will be considered to be infinite.

In the case of the component, $R_m$, the value, when measured, is significant, (In these transducers the values ranged from nine to sixty ohms). It had been the opinion of the writer that in the vicinity of resonance the value could be measured, and the measured value could be used in equivalent circuit calculations. However, as reported in Sections 5 and 6, the resistance at resonance was observed, under certain conditions, to change 138%.

The equation for $C_o$ is the form for a system of 28 identical capacitors connected in parallel. $C_o$ is given as follows:

$$C_o = \frac{n\ (\epsilon_o)(\epsilon_y')(S_y)}{4\pi\ (l_y)} \qquad (1)$$

Where:

| | |
|---|---|
| $S_y$ | is the plated area of one single bar |
| $n$ | is the number of bars |
| $\epsilon_y'$ | is the clamped dielectric constant of the Lead Zirconate-Titanate |
| $\epsilon_o$ | is the permittivity of free space |
| $l_y$ | is the mean length of the arc between the plates of one segment. |

In deriving the algebraic expression for the remaining components of the equivalent circuit, each component involves a transformation factor. Therefore the derivation of the transformation factor will be discussed prior to continuing with the derivation for the other components.

The transformation factor is defined[1] as the quantity relating the piezo-electrically generated current in the short circuited electrical side of the transducer, ( E = 0 ) to the generating velocity, ( U ) in the mechanical side. This gives the ratio of coulombs per second divided by meters per second, or just coulombs per meter. This is equivalent to the total charge displaced divided by the radial displacement.

The basic equation for the charge density [2] of a transducer is:

1. L.E. Kinsler, A.R. Frey, "Fundamentals of Acoustics", Second edition John Wiley & Sons, p 343.
2. Ibid. equation 12.1, p 335

$$\sigma_y = \frac{(\epsilon_y')(\epsilon_o)(E_y)}{l_y} - \frac{(d_{33})(n)(F_y)}{S_y} \qquad (2)$$

But since for the purposes of this derivation the potential across the transducer is zero, this reduces to:

$$(\sigma_y)(S_y) = (-d_{33})(n)(F_y) \qquad (3)$$

To obtain the displacement of the transducer it is necessary to take the equation [1] relating stress, strain, and piezo-electric activity in a transducer, solve for strain and then multiply both sides of the equation by the length of the transducer in the direction of its primary motion.

$$\frac{\partial \eta}{\partial y} = \frac{(S_{33})(F_y)}{S_y} + \frac{(d_{33})(E_y)}{l_y} = -\frac{(S_{33})(F_y)}{S_y} \qquad (4)$$

After multiplying by the mean circumference of the cylinder the circumferential displacement is:

$$\xi_c = -(l_y)(S_{33})\frac{(n)(F_y)}{S_y} \qquad (5)$$

But the radial displacement is related to the circumferential displacement by a factor of $(2)(\pi)$. Therefore;

$$\xi_r = -(l_y)(S_{33})(n)\frac{(F_y)}{(S_y)(2)(\pi)} \qquad (6)$$

Equations three and six may be used in the definition given above and the result is an expression for the transformation factor.

$$\Phi = \frac{(\sigma_y)(S_y)}{\xi_r} = \frac{(2)(\pi)(d_{33})(S_y)}{(S_{33})(l_y)} \qquad (7)$$

1. Ibid. equation 12.2, p 335.

Where: $S_y$ is the plated area of one bar
$d_{33}$ is the piezo-electric constant
$S_{33}$ is the elastic compliance
$l_y$ is the mean length of the arc between the plates of the segment

The motional inductance of a transducer is defined [1] as the effective mass divided by the square of the transformation factor. As a result of the configuration the entire mass of the transducer is the effective mass.

$$L = \frac{M}{\Phi^2} = \frac{(\rho)\,(R_1^2 - R_2^2)\,(\pi)\,(h)}{\Phi^2} \qquad (8)$$

Where: $\rho$ is the density of the material
$R_1$ is the outside radius
$R_2$ is the inside radius
$h$ is the height of the transducer

The motional capacitance , C , is defined [2] as the square of the transformation factor divided by the effective stiffness of the transducer. In this particular transducer the effective stiffness is the radial stiffness or the change in radius for a given applied external force. In this portion of the derivation it is assumed that the transducer is located in air so that the medium exerts very little influence upon the stiffness of the transducer.

The short-circuited stiffness of a segment in the parallel mode is:

$$S = \frac{-F_y}{l_y} \qquad (9)$$

From equation six the displacement as a function of crystal dimensions and constants may be derived so that:

$$S = \frac{(2)\,(\pi)\,(S_y)}{(S_{33})\,(l_y)\,(28)} \qquad (10)$$

1. Ibid. p 345
2. Ibid. p 345

Equation ten represents the circumferential force generated for a unit radial compression. The equation of interest is the radial force generated for a unit of radial compression. By examining the geometry of the individual segment (see Fig. 6 ) the radial force acting on the segment may be related to the circumferential force by equation eleven.

$$F_c = \frac{1}{2} (F_r) \left(\frac{1}{\text{sine } \frac{\theta}{2}}\right) \qquad (11)$$

where the angle $\theta$ is the angle subtended by the arc of one segment.

In this particular case the angle $\frac{\theta}{2}$ , is small enough so that the sine of the angle may be replaced by the angle expressed in radians. Now the radial force may be written as:

$$F_r = (\theta)(F_c) = \frac{(2)(\pi)(S_y)(R)(\theta)}{(28)(S_{33})(I_y)} \qquad (12)$$

But:

$$\theta = \frac{(28)(I_y)}{(R)} \qquad (13)$$

so that:

$$F_r = \frac{(2)(\pi)(S_y)}{(R)(S_{33})} \qquad (14)$$

and:

$$S = \frac{-F_r}{R} = \frac{-(2)(\pi)(S_y)}{(R)(S_{33})} \qquad (15)$$

Thus, the motional capacitance is given:

$$C = \frac{-(\Phi^2)(R)(S_{33})}{(2)(\pi)(S_y)} \qquad (16)$$

Where: $S_y$ is the plated area of one segment

$S_{33}$ is the elastic compliance coefficient

R is the mean radius of the cylinder

The radiation impedance for this free flooding transducer in water is complicated by the fact that the sound field generated is the result of coupling to the medium from both the exterior and interior of the cylinder.

It was assumed that the exterior loading of the cylinder could be approximated by multiplying the radiating area by the specific acoustic impedance[1]. This expression is given in equation 17.

$$Z_c = (A_o)\,(C_m)\,(\rho_o)\left(\frac{1}{1+\left(\frac{1}{2ka}\right)^2} + j\,\frac{\frac{1}{2ka}}{1+\left(\frac{1}{2ka}\right)^2}\right) \qquad (17)$$

The interior loading was emperically determined from experimental data to be equivalent to a capacitive reactance of 1.96 ($10^3$) ohms. An explanation for this type of reactance loading has been given by Robey.[2] It should be noted that in both of the works cited the derivations were based on infinitely long cylindrical transducer. Therefore the use of these two sources is only an approximation to what actually occurred.

1. T.F. Hueter, R. H. Bolt, "Sonics", John Wiley & Sons, New York, 1955.
2. D. H. Robey, "On the Contribution of a Contained Viscous Liquid to the Acoustic Impedance of a Radially Vibrating Tube", Jour. Acoust. Soc. Am., Vol 27, No. 1, pp 22-25, Jan. 1955.

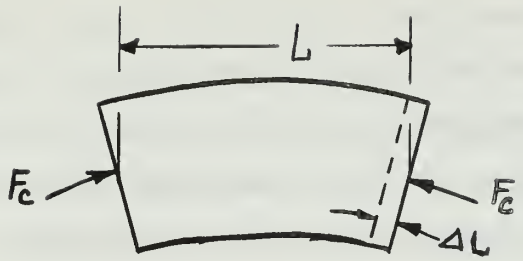


Figure 5. Circumferential Stiffness in the ceramic Segment.

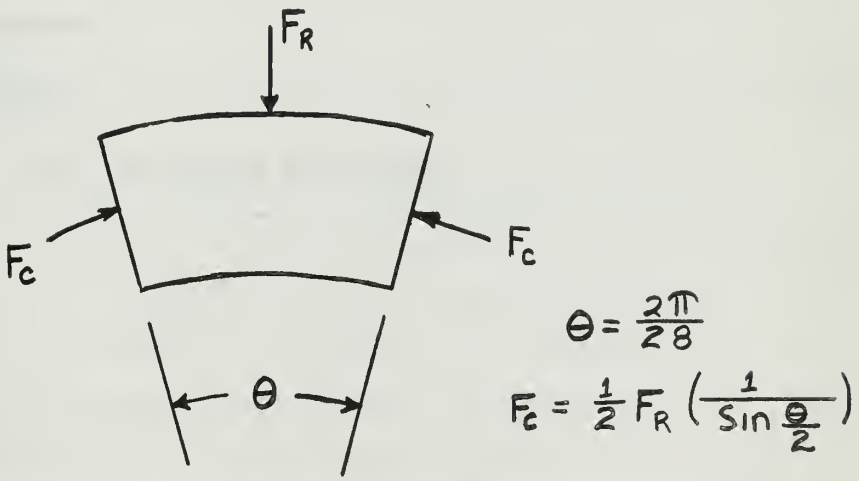


Figure 6. Force diagram in the ceramic segment.

4. Changes in Transducer Resonant Frequency and Quality Factor, Q, During Construction.

When possible during construction, low power admittance loops were taken in an attempt to observe the effects of the construction process on the resonant frequency and on the Q of the transducer. The general result of these observations is contained in Table I. Also found in Table I are the comparable values computed from the equivalent circuit parameters of Section 3.

The remainder of this section will be utilized to rationalize these changes, and to compare them to results computed by the Control Data Corporation 1604 Digital Computer using the program contained in Appendix I.

The resonant frequency of the transducer is that frequency at which there is maximum conductance. When the transducer is air loaded this corresponds to the frequency at which the negative susceptance resulting from the mass of the transducer is equal in magnitude to the positive susceptance resulting from the stiffness of the cylinder.

$$(\omega_r)\ (C) = \frac{1}{(\omega_r)\ (L)}\ , \tag{18}$$

or

$$\omega_r = \sqrt{\frac{1}{(C)\ (L)}}\ . \tag{19}$$

The quantities L, and C may be expressed:

$$L = \frac{M}{\Phi^2} \tag{20}$$

and:

$$C = \frac{\Phi^2}{S}\ . \tag{21}$$

Therefore, the air loaded resonant frequency may be expressed:

$$\omega_r = \sqrt{\frac{1}{\frac{M}{S}}} = \sqrt{\frac{S}{M}} \tag{22}$$

So it is seen that in air a change in transducer resonant frequency may be expressed as a change in the effective mass or effective stiffness of the cylinder.

As increase in resonant frequency of 0.326 percent was observed when the corners of the 28-sided polygon were sanded off. From Table I it is seen that the mass, transformation, factor, blocked capacitance, motional inductance, and motional capacitance all decrease as a result of the dimensional changes involved. The motional inductance and motional capacitance are the only members of the above list which will effect the resonant frequency and the decrease observed in both tends to increase the resonant frequency. The rise in resonant frequency was computed and experimentally observed. The drastic change in the computed version was caused by the assumption in the computer model that the outside of the transducer was a perfect cylinder.

As a result of sanding the cylinder, the Q of the transducer was observed to drop. It is the opinion of the writer that this drop in Q is caused by the fact that the circumferential forces which were originally applied over an area (t) (h) is now applied to an area $(R_1 - R_2^2 + (\frac{l_y}{2})^2)(h)$. This reduction in area causes an increase in stress magnitude in the lossy adhesive material.

In the computer model the Q rose from a low level to a level comparable to the observed value.

The addition of the fiberglass during prestressing caused the following changes: Mass, compliance, blocked capacitance, and the motional inductance increase in magnitude while the transformation factor, and motional capacitance decrease in magnitude. The increase in mass tends to decrease the resonant frequency while the decrease in motional capacitance would tend to raise it. The resonant frequency in this stage of construction was observed to increase, where as in the computer model the resonant frequency decreased. It is believed that an error was made in choosing the values of density and compliance of the fiberglass for the

computer model, causing the disagreement between the model and the experiment.

Table I

| Parameter | Rough | Sanded | Prestressed | Potted | Loaded | Loaded* |
|---|---|---|---|---|---|---|
| Resonant frequency | 8289 | 8325 | 8587 | 7833 | | 9117 |
| % change | -- | 0.32 | 3.13 | -8.79 | | 16.4 |
| Computed resonant frequency | 8703 | 9835 | 8651 | 7243 | 6786 | 8717 |
| Quality factor | 322 | 222 | 292 | 74 | | 3 |
| % change | -- | -30 | 30 | -74 | | -96 |
| Computed quality factor | 183 | 240 | 505 | 105 | 1.98 | 2.44 |
| mass (kgs) | 1.83 | 1.37 | 1.45 | 2.69 | 2.69 | 2.69 |
| Compliance ($10^{-11}$) | 1.32 | 1.32 | 1.33 | 1.33 | 1.33 | 1.33 |
| Transformation factor | 5.16 | 4.93 | 4.27 | 5.34 | 5.34 | 5.34 |
| $R_o(10^{150})$ | 1 | 1 | 1 | 1 | 1 | 1 |
| $C_o(10^{-10})$ | 9.40 | 7.98 | 8.02 | 10.04 | 10.04 | 10.04 |
| R | 19.9 | 14.0 | 7.91 | 40.19 | 40.19 | 40.19 |
| Inductance ($10^{-3}$) | 68.6 | 56.3 | 79.8 | 94.3 | 94.3 | 94.3 |
| Capacitance ($10^{-9}$) | 4.87 | 4.64 | 4.24 | 4.27 | 4.27 | 3.24 |

Figure 7 A tabulation of transducer parameter changes as a function of construction steps.

*A second computer run was made with an empirical correction added for internal radiation impedance.

When the transducer was potted the following parameters increased: Mass, transformation factor, blocked conductance, motional inductance and motional capacitance. An increase in motional inductance and motional capacitance would cause a decrease in resonant frequency. The computed change is so large because of the assumptions made concerning the density and compliance of the potting material. The observed and computed values of Q dropped because of the large increase in observed losses at resonance.

One of the most interesting parts of this study was the change of resonant frequency which accompanied the immersion of the transducer into a 30' by 30' by 8' concrete water filled tank[1]. The resonant frequency rose from 7833 to 9117 cycles per second. The only plausible cause of this change in resonant frequency has been explained[2] as being the result of the interior loading of the transucer. The waves generated by the interior wall of the cylinder, strike the opposite wall of the cylinder generally out of phase with the vibrations in that wall. This mutual loading may cause the motional impedance to be pure resistive, resistive and capacitive, or resistive and inductive depending upon the frequency at which the transducer is driven. For this type of radiation the $R_m$ in the equivalent circuit must be replaced by $Z_m$. It is assumed that the radiation impedance is composed of a contribution from equation 17 plus a frequency dependent term arising from the interior loading. It was not feasible to solve for the interior loading, however, by making calculations from the observed data, the reactance required to produce the observed change in resonant frequency, was computed to be $-j1.96(10^3)$ ohms. This is equivalent of inserting a $8.9(10^{-9})$ farad capacitor in series in the motional loop.

1. At first thought one might conclude that the standing waves set up in the tank would cause the changes observed. To determine the effect of the tank a duplicate set of tests on one transducer was conducted on a barge anchored in Lake Cayuga, New York. No differences in results were detected.
2. Robey; Op. Cit.

The computer model was solved twice for this step in construction. The first time the only loading considered was that due to the exterior loading. The resonant frequency was observed to decrease. On the second try an arbitrary capacitor of value $8.9(10^{-9})$ farads was introduced into the motional branch. This caused a significant rise in the resonant frequency of the model.

The Q of the transducer dropped drastically as a result of the water loading. This change in Q was also observed in the computer model, for both solutions. This tends to substantiate the conclusion that the interior by the acoustic impedance as seen by the exterior surface of the transducer.

During the tests the changes in resonant frequency for each step of construction were quite uniform in direction and magnitude for all of the transducers. However such is not the case in the observations of Q. From data collected on six transducers, three of them changed in direction and magnitude in the same manner as listed in the table in Fig. 7. For two of the other three the changes in Q were very slight. This is attributed to a different adhesive used in one of the two, and perhaps differences in curing and removing of mass when the cylinder was rounded. For the third the rise of resonant frequency with prestressing caused a spurious resonant loop to be included between the half power points significantly increasing the bandwidth and decreasing the Q.

5. Changes in Transducer Parameters as a Function of Temperature.

During the process of testing the transducers it was noted that as a result of internal dissipation, the temperature of the transducer was raised. It was determined that the effects of the change in temperature on this transducer were quite marked. To determine the extent of these effects the following procedures were used:

a. A thermocouple was mounted in the ceramic to monitor the transducer temperature.

b. The transducer was driven at various temperature levels with a constant input power to minimize the effects of dynamic stress.

c. The input voltage and current were displayed on an oscilloscope in a Lissajous pattern. This figure was used to determine the resonant frequency. The voltage and current were also measured with a vacuum tube voltmeter. The arrangement of the test equipment is shown in Fig. 8.

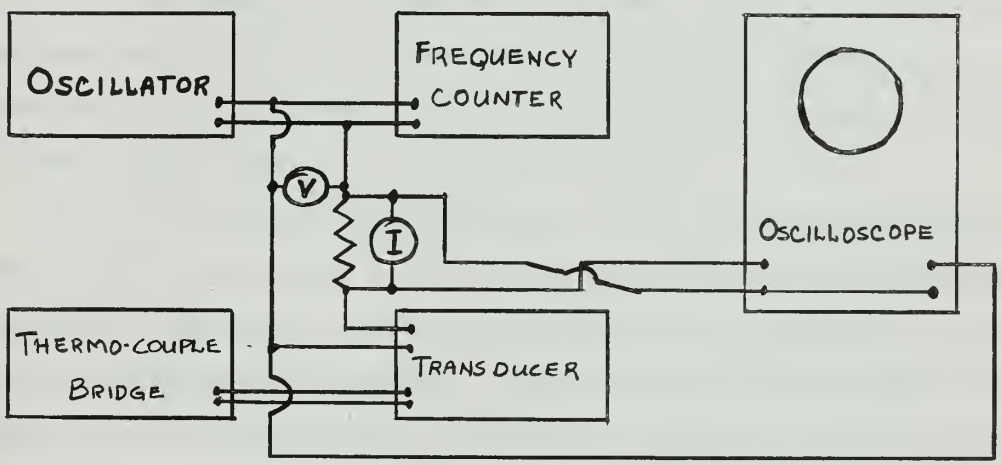


Figure 8. Test equipment for investigation of temperature effects in the cylindrical transducer.

The fact that the transducer, when driven at high stress levels, became hotter was used to provide the elevated temperatures required for the test.

Some of the results of these tests were:

a. At a temperature of about 60°C the transducer exhibited a change in the trend of resonant frequency as a function of temperature. As the temperature was increased from room temperature, the resonant frequency rose almost linearly until a temperature of 55° was reached. From a temperature of 65° to 105° (the limit of the test) the resonant frequency dropped almost linearly with temperature. The tests were conducted with temperature changes in both directions, but little or no hysteresis effect was noticed. The resonant frequency increase observed in the lower temperature range, represented a change of .827 percent while the decrease, above 60°C. was a change of -1.415 percent. The data from these experiments are plotted in Fig. 9 .

Some additional measurements were made utilizing a constant driving potential. The measurements of impedance at resonance versus temperature again revealed the apparent change at 60°C. From room temperature to 60° the impedance was relatively constant. After 60° the impedance rose markedly. At a high drive level the change in impedance was observed to be 61 percent, while at a low level the change was 138 percent. These results are plotted in Fig. 10.

To the writer the next logical step in this investigation would have been to take a single bar of PZT-4 and conduct similar experiments to determine if the effects could be attributed to the ceramic or to the rather complex prestressed transducer. Unfortunately the only PZT-4 ceramic bars available were plated on sloping sides which in itself might be sufficient to induce some peculiarities into the results. In addition the bar would have to be driven in a mode quite different to that in which it was excited as part of the composite transducer. To drive one of the bars in the parallel mode the frequency required would have been 248 kilocycles per second. This frequency was well beyond the capabilities of the test equipment. Due to the delay involved from the time of placing an order until the time of receipt of a special test bar, the writer was unable to continue this experiment to its conclusion.

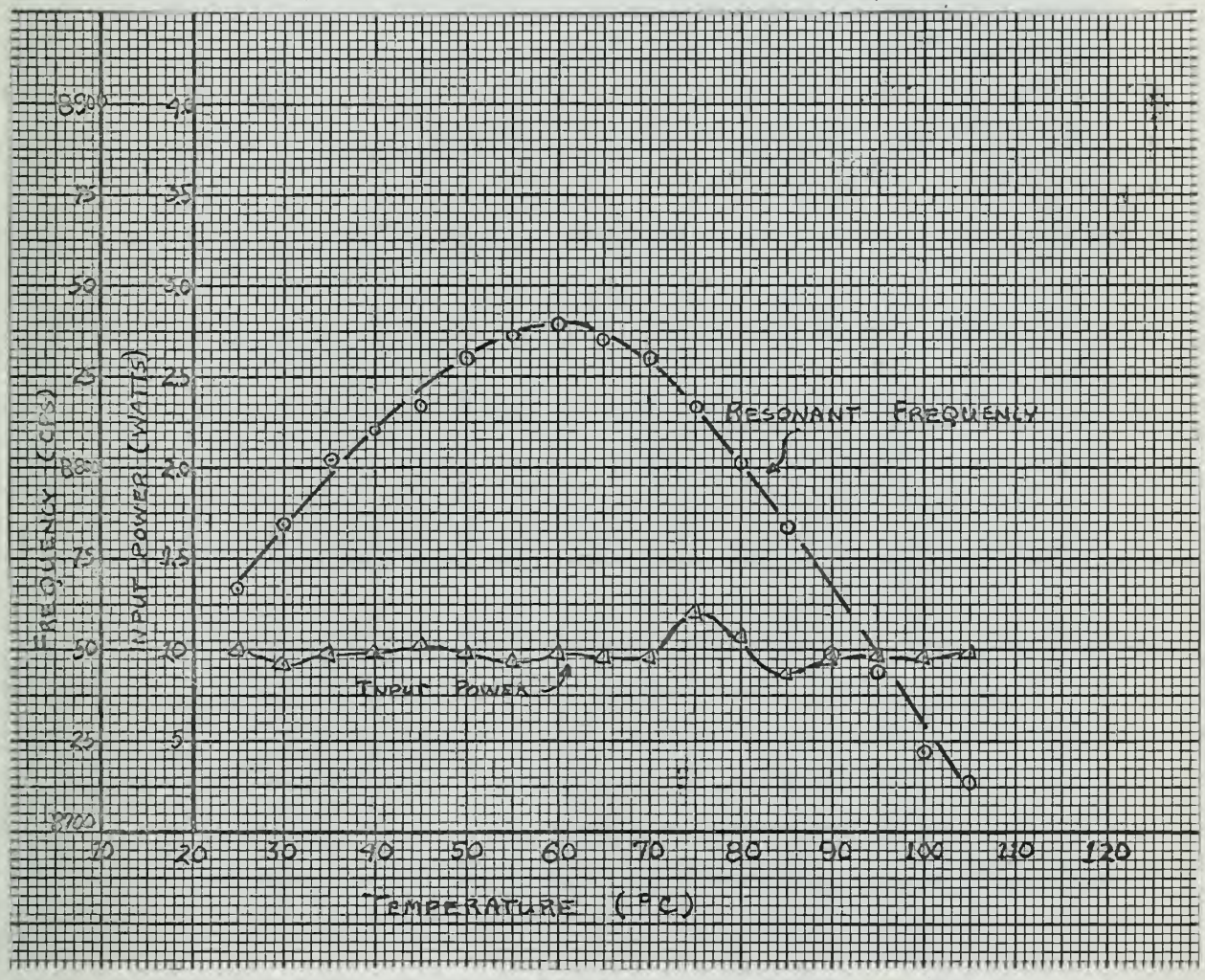


Fig. 9 Resonant frequency of segmented cylindrical transducer versus temperature.

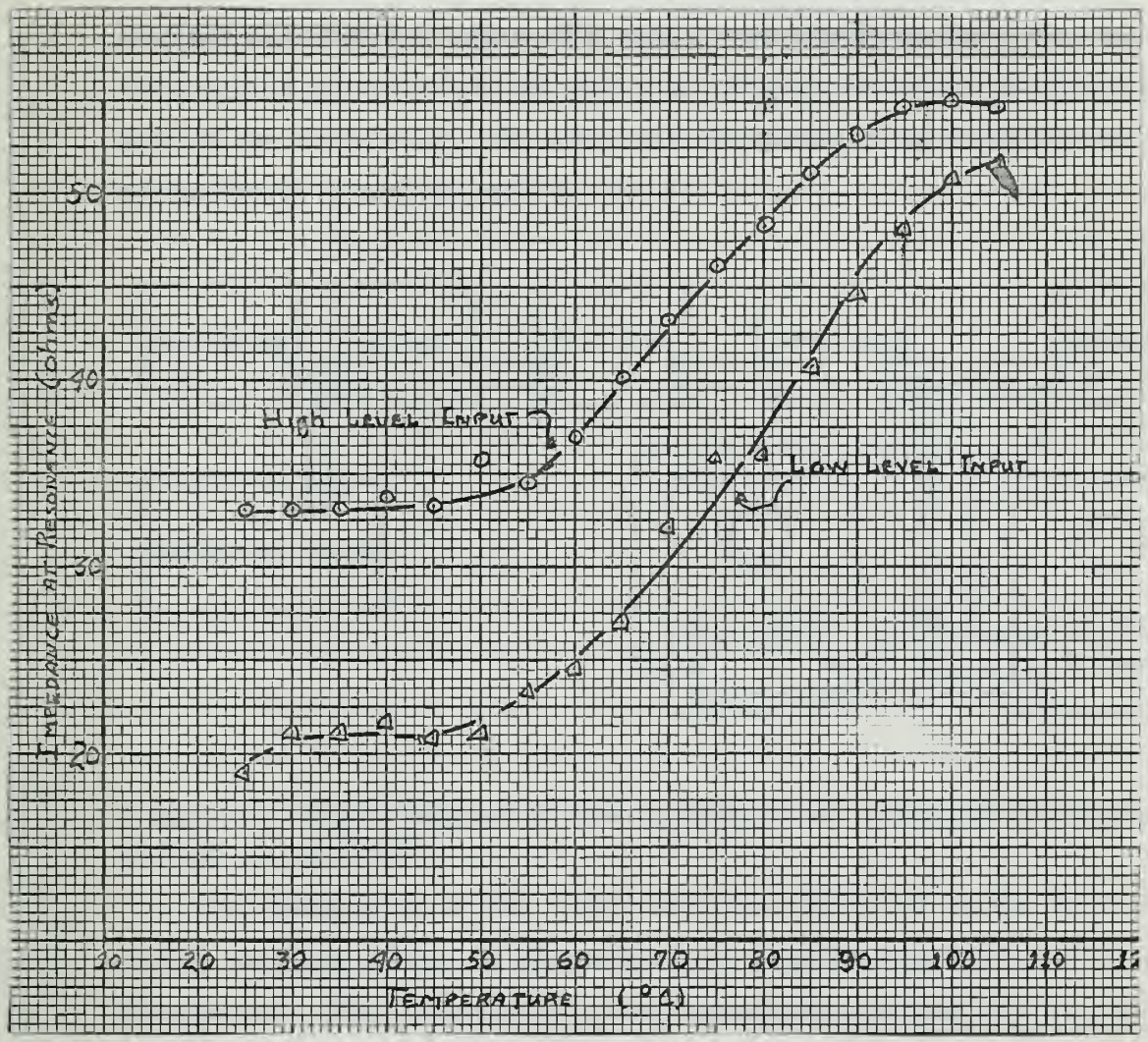


Fig. 10 Impedance at resonance of a segmented cylindrical transducer versus temperature.

6. Changes in Resonant Frequency and Impedance at Resonance as a Function of Dynamic Stress.

Using pulse techniques (to reduce temperature drift as a result of internal dissipation) with a 200 watt power amplifier, data was taken for the purpose of analyzing the effect of dynamic stress on the characteristics of the transducer. The test was conducted using facilities as depicted in the block diagram in Fig. 11.

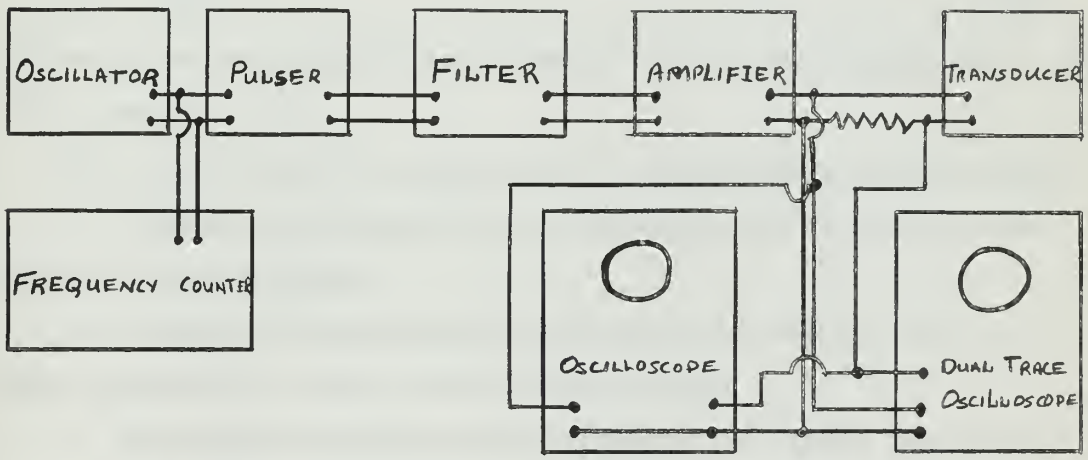


Figure 11. Block diagram of test equipment for parameter measurements at high stress level.

The temperature of the transducer was monitored during the test to insure that the effects of temperature as described in Section 5 could be discounted. The temperature of the transducer changed two degrees Centigrade over a period of two hours of testing.

The data taken during these tests were:

a. Transducer input voltage

b. Transducer input current

c. Resonant frequency

d. Half power points

From these data the internal stresses were calculated as well as the change in Young's Modulus, and Q. When the change in Young's Modulus was plotted versus stress the results substantiated the work of Robert

Gerson[1], (see Fig. 12). In his paper, Gerson discusses the effect of the stress on the Q of the transducer. This effect was also observed by the writer, but the writer postulates that the change in Q is a result of a change in more basic quantities in the transducer, such as changes in R, $Y_{33}$, and resonant frequency. When the Q of the transducer was computed using the equivalent circuit parameters and those parameters which were observed to change with stress, using the equation:

$$Q = \frac{\omega_R L}{R} \tag{35}$$

The resultant curve closely approximated the observed experimental data for Q, (see Fig. 13).

The methods used for taking data for these tests were as follows:

a. Voltage was displayed on an oscilloscope and peak to peak quantities were measured.

b. Current was determined by measuring the voltage drop in a series connected 0.1 ohm non-inductive resistor.

c. The resonant frequency was measured by using a frequency counter and setting the frequency generator by obtaining a Lissajous pattern between current and voltage. When the current and voltage were in phase the transducer was considered to be operating at its resonant frequency.

d. The half power points (measured with the transducer in air) were determined by using a calibrated marker on the oscilloscope to offset the current wave form from the voltage wave form by plus and minus 45 degrees. The error in determining the half power point by this method was estimated by the writer to be less than five degrees. In taking this type of measurement there is one serious defect which may effect the validity of the measurements. When the transducer is driven at the half

1. Robert Gerson, Op. Cit.

power points the stress level is much lower than that which is experienced at resonance. Since the values under measurement do change as a function of stress level it is inconceivable to the writer that this effect would not induce error in the results. The solution to this problem may be to drive the transducer mechanically at the desired stress level at the frequency of measurement.

As a result of the complexity of the transducer under test, the writer was unable to determine the causes of these effects (i.e. Were the effects a characteristic of the ceramic, or a quirk of construction?)

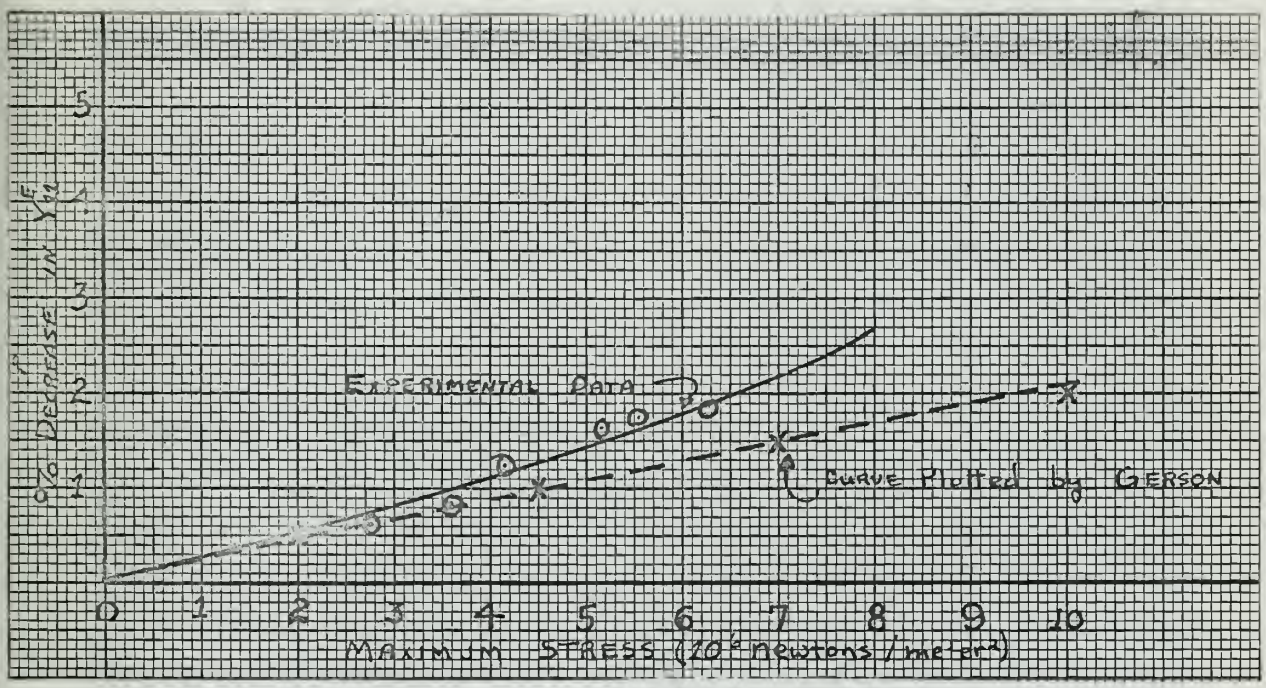


Fig. 12 Change in Young's Modulus versus stress.

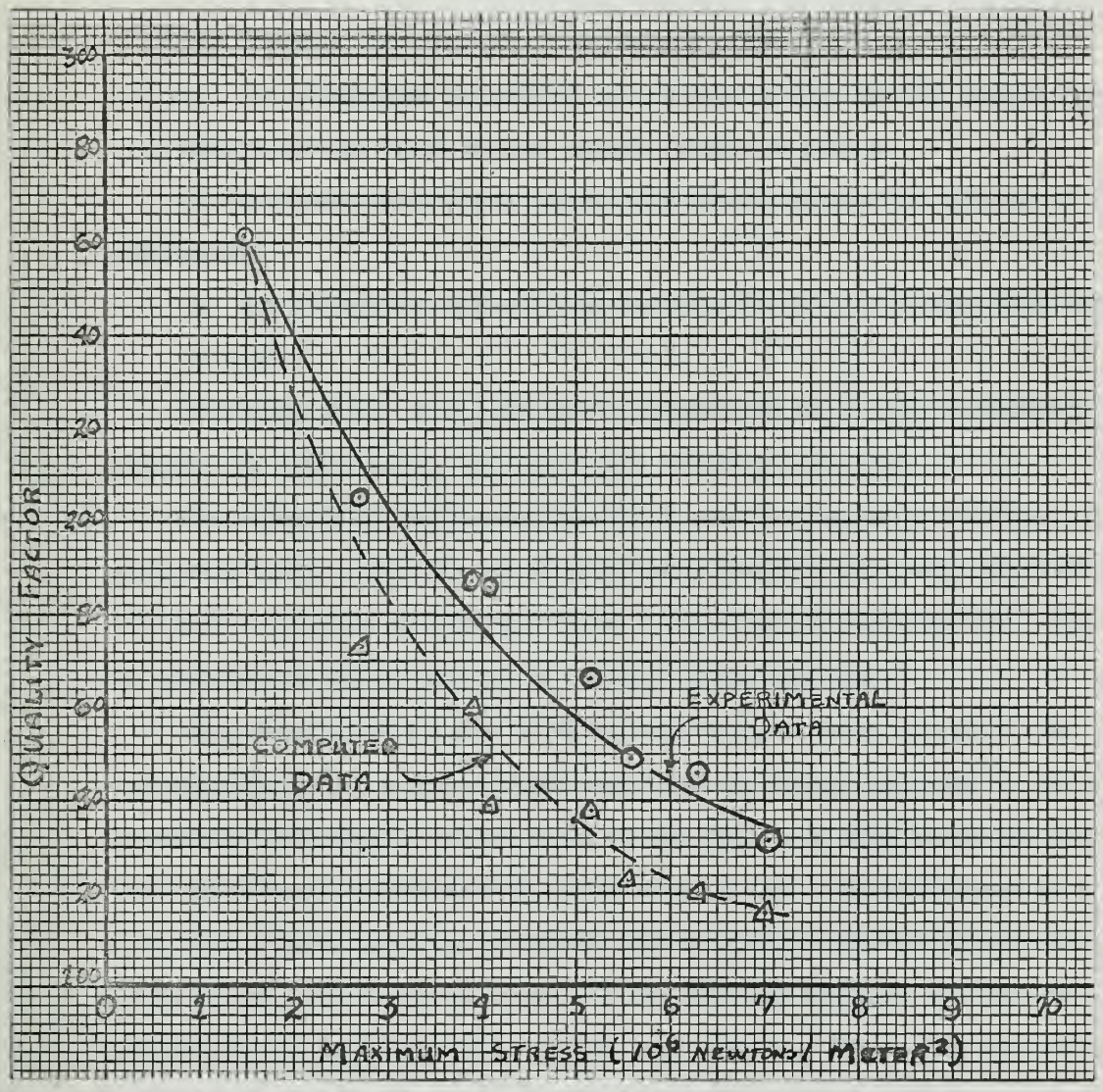


Fig. 13 Measured parameters versus stress level.

7. Discussion and recommendations.

The two major objectives of this experiment were:

a. To drive the transducer to an acoustic output of fifteen watts per square centimeter of radiating area.

b. To determine the effect of stress levels on the transducer when driven at the high output level stated in part a.

A secondary objective presented itself during the course of the expriment:

c. To determine the effects of temperature on transducer parameters.

Although none of these three objectives was fully achieved, the results do allow some comment and recommendations.

The effects of temperature which are discussed in Section Five were shown to exist, yet the equipment and transducers were not available to allow a pursuit of this problem to its logical conclusion. This inquiry is considered to be worthy of further investigation.

The effects of stress level in the ceramic was shown to be substantially the same as that reported by Robert Gerson[1]. In an effort to extend the experimental data to the limits of the prestress level, the test transducer developed a crack around the circumference at a circumferential stress level well below the maximum design stress level. Apparently, the third harmonic of the driving voltage excited the longitudinal resonant mode of the transducer. Since the transducer prestressing treatment was not effective for longitudinal stresses, the breaking stress for this direction should be significantly smaller than for the circumferential direction.

As in the case of the temperature effects the effects of dynamic stress on the transducer is considered to be worthy of further investigation. Some recommendations for improving these two experiments are:

a. The test transducers should be simple PZT-4 ceramic bars.

1. Gerson Op. Cit.

b. Pulse techniques should be used to eliminate the possibility of significant dynamic heating.

c. A dual trace Memo-scope should be used for current and voltage measurements when using pulse techniques. The resonant frequency may be found by using a Lissajous pattern on a separate oscilloscope.

d. In the experiment concerning the effects of temperature, it is recommended that a calibrated and controlled oven be used as a heat source instead of relying on the dynamic heating of the transducer.

e. In the experiment concerning the effects of stress level, it is recommended that measurements be made at much higher stress levels. Care should be used to insure that the input is well filtered to prevent recurrence of the previous transducer failure.

It is the contention of the writer, that the transducers are not as uniform in their properties as they should have been. The following changes in construction techniques are recommended as possible methods in which the uniformity of the product may be improved:

a. Do not cure the Epon Cement holding the bars until after the transducer has been prestressed. This should tend to make the cement joints more uniform in thickness.

b. During the curing process the transducer should be driven at a moderate level to allow the static stresses in the transducer to become evenly distributed, and perhaps to eliminate the conditions which gave rise to the spurious resonances observed in several of the transducers.

c. The use of an adhesive should be kept to a minimum. The prestress should maintain the integrity of the device, therefore the adhesive is effective only in filling the voids between segments.

d. The segments should be formed as segments of a cylinder instead of truncated prisms. This would eliminate the sanding operation

and perhaps reduce the losses of the transducer because the forces acting on the joints would be acting over a larger area and therefore the stress amplitude in the joint would be lessened.

BIBLIOGRAPHY


1. D. Berlincourt, B. Jaffe, H. Jaffe, and H. H. A. Krueger, "Transducer Properties of Lead Titanate Zirconate" IRE transactions on Ultrasonics Engineering, Vol UE-7, No. 1, pp 1-6, Feb 1960

2. L. E. Kinsler, A. R. Frey, "Fundamentals of Acoustics" Second edition, John Wiley & Sons, Inc., New York, New York, July 1962

3. A. Kremheller, "Ferroelectric Materials and their Applications" Sylvania Technologist Vol 13, No. 2, pp 42-48, April 1960.

4. A. Kremheller and P. W. Renaut, "Ferroelectric Ceramics" Sylvania Technologist, Vol 13, No. 3, pp 82-89, July 1960.

5. R. Gerson, "Dependence of Mechanical Q and Young's Modulus of Ferroelectric Ceramics on Stress Amplitude" Journal of the Acoustical Society of America Vol 32, No. 10, pp 1297-1301, October 1960.

6. D. Berlincourt, "Power Capacities of Piezoelectric Ceramics in Sonar Type Acoustic Transducers", Clevite Corporation, Technical paper, TP-221, July 1961.

7. D. H. Robey, "On the Contribution of a Contained Viscous Liquid to the Acoustic Impedance of a Radially Vibrating Tube", The Journal of the Acoustical Society of America, Vol 27, No. 1, pp 22-25, January 1955.

8. W. P. Mason, "Piezoelectric Crystals and their Applications to Ultrasonics", D. Van Nostrand Co., Inc., New York, New York, 1950.

9. T. F. Hueter, R. H. Bolt, "Sonics" John Wiley and Sons, New York, 1955.

Appendix I Computer Program for Solution of the Admittance Problem of a Segmented Cylindrical Transducer

A Fortran program was written for the Control Data Corporation 1604 digital computer, to solve for admittance versus frequency for a cylindrical segmented prestressed transducer. The program is composed of a driving routine and two subroutines.

The driving routine proposes the problem to be solved by the two subroutines. It is written as six consecutive problems with only those dimensions and constants changed in each problem as dictated by the construction process.

The first subroutine computed arguments for the second subroutine from data supplied by the driving routine. These calculations were the ones which were common to each of the six problems.

The second subroutine took the arguments from the first subroutine and computed resonant frequency, half power points, quality factor, motional conductance, motional susceptance, total conductance, total susceptance, and magnitude of the total admittance.

The frequency increments used are computed using the scheme based of the half band width of the transducer. The numbers of cycles per increment is dependent upon the number of half bandwidths that the frequency is away from the resonant frequency: The nearer the resonant frequency, the smaller the increment. Since the increment is in effect, based on Q., no matter how high or low the Q, there will be a sufficient number of points computed in the vicinity of resonance to insure satisfactory plot of susceptance versus conductance.

The assumptions used in the solution to this problem are:

a. The cylinder is sanded from a perfect 28-sided polygon to a perfect cylinder.

b. The adhesive material is of the same density as the ceramic.

c. The adhesive joint is 0.001 meters thick.

d. The density of the fiber glass is 1800.0 kgs/meter$^3$.

e. The compliance of the fiber glass is the same as that for glass.

f. The density of the potting compound is the same as that of soft rubber.

g. The compliance of the potting compound has no effect on the stiffness of the transducer.

h. The interior loading i air is neglected.

The program was as follows:

```
..JOB*UNDERWOOD8 F.S. BIN 93
      PROGRAM IMPEDANCE
      CME = 1.0E150
      PI = 3.1415927
      RHOM = 1.21
      VEL = 3.43E2
      T = 0.0085
      XH = 0.076
      RHO = 7500.0
      S33 = 1.32E-11
      S = S33
      RO1 = 0.0604
      RI1 = 0.05192
      XLYO1 = 0.0135
      XLYI1 = 0.0115
      XLY = (XLYO1 + XLYI1)/2.0
      AHIG = XH
      RAD = RO1
      G1 = 0.049
      G2 = 0.069
      G3 = 0.1165
      G4 = 0.0245
      XM1 = T*XH*RHO*(28.0*XLY + 0.028 )
```

```
RM1 = (RO1 + RI1)/2.0

T2 = T

CALL COMPUTE (S,T,XH,XLY,XM1,G1,RM1,T2,RHOM,VEL,
                RAD,AHIG,CME)

T2 = RO1 - SQRTF(RI1**2 + XLYI1**2)

TM = T2 + 0.707*(T-T2)

RM2 = RI1 + TM/2.0

DXM2 = 14.0*RO1*XH*(XLYO1 + 0.001) - XH*PI*(RO1**2)

XM2 = XM1 - DXM2*RHO

CALL COMPUTE (S,TM,XH,XLY,XM2,G2,RM2,T2,RHOM,VEL,
                RAD,AHIG,CME)

RO3 = 0.062

RHOG = 1800.0

XMG = RHOG*XH*(RO3**2 - RO1**2)*PI

XM3 = XM2 + XMG

S3G = 1.0/(6.2E10)

TM3 = 0.707*(RO3-RI1)

RAD = RO3

RM3 = RI1 + TM3

CALL COMPUTE (S3G3,TM3,XH,XLY,XM3,G3,RM3,T2,RHOM,
                VEL,RAD,AHIG,1CME)

DT = (3.0/8.0)*2.54*0.01

RO4 = RO3 + DT

RI4 = RI1 - DT
```

```
XH4 = XH + 2.0*DT

RHOP = 1630.0

RAD = RO4

SP = 1.0/(0.0005E10)

VT = XH4*PI*(RO4**2 - RI4**2)

VI = XM2/RHO + XMG/RHOG

VP = VT - VI

XMP = VP*RHOP

XMP4 = XM3 + XMP

SP4 = S3G3

RM4 = (RO4 + RI4)/2.0

AHIG = XH4

CALL COMPUTE (SP4,TM3,XH4,XLY,XMP4,G4,RM4,T2,RHOM,
              VEL,RAD,AHIG,1CME)

RHOM = 1000.0

VEL = 1500.0

CALL COMPUTE (SP4,TM3,XH4,XLY,XMP4,G4,RM4,T2,RHOM,
              vel,rad,ahig,1CME)

CME = 8.9E-9

CALL COMPUTE (SP4,TM3,XH4,XLY,XMP4,G4,RM4,T2,RHOM,
              VEL,RAD,AHIG,1CME)

END
```

```
      SUBROUTINE COMPUTE (S,T,XH,XLY,XM,G,RM,T2,RHOM,
     1                    VEL,RAD,AHIG,CME)
5     FORMAT (4H XL )
6     FORMAT (4H C )
      AHIG        = AHIG
      RHOM = RHOM
      VEL = VEL
      RAD = RAD
      PHO = 1.21
      PVL = 343.0
      D33 = 2.1E-10
      EPO = 8.85E-12
      EPY = 1300.0
      PI = 3.1415927
      XK = SQRTF (D33**2/(EPO*EPY*S) )
      EPYC = EPY*(1.0-XK**2)
      CO = (7.0*EPO*EPYC*T2*XH)/(PI*XLY)
      RO = 1.0E150
      PHE = (2.0*PI*D33*T*XH)/(S*XLY)
      PHESQ = PHE**2
      XL = XM/PHESQ
      R = 1.0/G
      ST = (2.0*PI*T*XH)/(RM*S)
```

```
      C = PHE**2/ST
      C = 1.0/(1.0/C + 1.0/CME)
      WO = SQRTF (1.0/(XL*C) )
      A = 2.0*PI*RAD*AHIG
      XWK = WO/PVL
      DA = 1.0 + 1.0/(2.0*XWK*RAD)**2
      RR = (A*PHO*PVL)/DA
      RR = RR/PHESQ
      R = R-RR
      RHOC = RHOM * VEL
      PRINT 7 , XM,S,  PHE
7     FORMAT (4H XM = 1PE11.4, 4H S = 1PE11.4, 6H PHE = 1PE11.4)
      CALL XDUCER1 (RO,CO,R.XL,C,RHOC,VEL,RAD,A,PHESQ)
      END
```

```
      SUBROUTINE XDUCER1 (RO,CO,R,XL,C,RHOC,VEL,
     RAD,A,PHESQ)
C     PROGRAM TO TEST MATHEMATICAL MODEL OF A CRYSTAL
C     VIBRATOR.  INPUTS REQUIRED ARE RO,CO,R,XL,C, (XDUCER
C     CONSTANTS), A(INITIAL FREQUENCY), DF (FREQUENCY
C     INCREMENT).
      DIMENSION YR(100),YI(100),YM(100),F(100),GM(100),
     BM(100),ZR(100), 1 ZI(100), ZBR(100),ZMR(100),
     ZMI(100),ZBI(100)
      PRINT 15
   41 CONTINUE
      PRINT 50, RO, CO, R, XL, C
      PRINT 15
      PRINT 51, RHOC, VEL,RAD,A
   50 FORMAT (4H RO = 1PE11.4,4H CO = 1PE11.4,3H R =
     1PE11.4,4H XL = 1PE11.14,3H C = 1PE11.4
   51 FORMAT (6H RHOC= 1PE11.4,5H VEL= 1PE11.4,5H RAD=
     1PE11.4,3H A = 11PE11.4)
      PRINT 15
   15 FORMAT(///)
      WO = SQRTF (1./(XL*C) )
      XK = WO/VEL
      RR= (A*RHOC)/(1.0 + 1.0/(2.*XK*RAD)**2)
```

```
      RR = RR/PHESQ
      RX =  R + RR
      Q = (WO*XL)/RX
      FO = WO/(2.*3.141)
      DEF = FO/(2.*Q)
      FB1 = FO - 2.*DEF
      FB2 = FO - DEF
      FB3 = FO -DEF/2.
      FB4 = FO + DEF/2.
      FB5 = FO + DEF
      FB6 = FO + 2.*DEF
      F(1) = FO - 10.*DEF
      K = 60
      F1 = FO - DEF
      F2 = FO + DEF
      DO 3  1 = 1,K
      IF (F(I) - FB1) 17,17,9
9     IF(F(I) - FB2) 18,18,12
12    IF(F(I)-FB3) 19,19,13
13    IF(F(I) - FB4) 21,21,14
14    IF(F(I)-FB5) 19,19,16
16    IF(F(I)-FB6) 18,18,17
```

```
18    DF = DEF/5.
      GO TO 2
19    DF = DEF/10.
      GO TO 2
21    DF = DEF/20.
      GO TO 2
17    DF = DEF
2     CONTINUE
      IF (F(I) ) 3,39,39
39    W = 2.*3.141*F(I)
      XK = W/VEL
      RR= (A*RHOC)/1.0 + 1.0/(2.*XK*RAD)**2)
      RR = RR/PHESQ
      XR=((A*RHOC)/(2.0*XK*RAD))/(1.0 + 1.0/(2.0*XK*
      RAD)**2)
      XR = XR/PHESQ
      AA = (R + RR)**2 + (W*XL - 1.0/(W*C) + XR)**2
      GM(I) = (R + RR)/AA
      YR(I) = 1./RO + GM(I)
      BM(I) = -(W*XL - 1.0/(W*C) + XR)/AA
      YI(I) = W*CO + BM(I)
      BB = YR(I)**2 + YI(I)**2
```

```
      YM(I) = SQRTF (BB)
3     F(I + 1) = F(I) + DF
      PRINT 6,FO,Q,F1,F2
      PRINT 60
60    FORMAT (13X,1HF  19X, 2HYR  17X,2HYI  17X,2HYM
      17X, 2HGM  17X,2HBM  //)
      PRINT 4 (F(I),YR(I),YI(I),YM(I),GM(I),BM(I),I=1,K )
4     FORMAT (6(1PE19.5) )
      PRINT 62
62    FORMAT (//)
      PRINT 15
10    CONTINUE
6     FORMAT (5H  FO= 1PE11.4,5H  Q= E11.4,5H  F1=
      E11.4, 1  5H  F2= E11.4)
69    CONTINUE
      END
      END


. .END
```